Front. Optoelectron. China 2009, 2(1): 113–117
DOI 10.1007/s12200-009-0006-z

RESEARCH ARTICLE

$Al_xGa_{1-x}N$ solar-blind photodetectors grown by low pressure MOCVD

Xiaoyan WANG (✉), Xiaoliang WANG, Baozhu WANG, Junxue RAN, Hongling XIAO, Cuimei WANG, Guoxin HU

Key Laboratory of Semiconductor Materials Science, Institute of Semiconductors, Chinese Academy of Sciences, Beijing 100083, China
Material Science Center, Institute of Semiconductors, Chinese Academy of Sciences, Beijing 100083, China

Abstract $Al_xGa_{1-x}N$ ternary alloys are very attractive materials for application to ultraviolet (UV) photodetection. In this work, high Al content $Al_xGa_{1-x}N$ films are grown on sapphire substrate by low pressure metalorganic chemical vapor deposition (MOCVD). The Al content in the $Al_xGa_{1-x}N$ epilayer is estimated to be 54% by high resolution X-ray diffraction (HRXRD) and Vegard's law. The full width at half maximum (FWHM) of the rocking curve for the $Al_{0.54}Ga_{0.46}N$ (0002) is about 597 arcsec. According to the transmittance measurement result, our sample is suitable for fabricating solar-blind photodetectors. The observed Fabry-Perot fringes in the transmission region indicate that high optical quality is obtained. Solar-blind metal-semiconductor-metal (MSM) photodetectors based on the MOCVD-grown $Al_{0.54}Ga_{0.46}N$ film are fabricated and tested. The detector has a low dark current of about 31 pA under a bias voltage of 5 V. An UV/visible contrast of about four orders of magnitude is observed and responsivity increases with increments of the bias voltage.

Keywords ultraviolet (UV) photodetection, metalorganic chemical vapor deposition (MOCVD), $Al_xGa_{1-x}N$, film, high Al content, metal-semiconductor-metal (MSM)

1 Introduction

III-V nitrides have recently attracted great interest for applications such as high temperature and high power microelectronic devices [1–8], ultraviolet (UV) light-emitting devices (LEDs) [9–13] and UV photodetectors [14–18]. UV photodetectors are a subject of increasing interest due to a variety of current and potential applications in the military, industrial and scientific areas. Some of these are covert space-to-space communications, early missile threat warning systems, jet engine monitoring, chemical/reagent detection, ozone and flame/engine monitoring and UV astronomy. Currently, Si-based detectors are employed in these applications. However, due to the narrow band gap of Si, these detectors require external filters that often reduce their efficiency levels 20% or lower. As a promising alternative to Si-based technology, detectors fabricated from III-nitride materials, in particular $Al_xGa_{1-x}N$, have been investigated and exhibited excellent potential. With a wide, direct band gap ranging from 3.4 to 6.2 eV, $Al_xGa_{1-x}N$ covers much of the UV spectrum. In particular, solar-blind photodetectors can be fabricated using $Al_xGa_{1-x}N$ films with $x > 0.45$ [19]. However, for many well-known reasons such as the increasing probability of pre-reactions and low surface mobility of Al-species [20], the growth of high quality $Al_xGa_{1-x}N$ with high Al composition poses extreme difficulty.

Due to fabrication simplicity, unnecessary p-type doping, as well as reduced parasitic capacitance and low dark current, a metal-semiconductor-metal (MSM) photodetector is an attractive candidate for high-speed photodetection. In this work, 1 μm-thick, high Al content $Al_xGa_{1-x}N$ films were obtained using ten pairs of AlN/$Al_xGa_{1-x}N$ superlattices (SLs) as a strain-management layer by low pressure metalorganic chemical vapor deposition (MOCVD). An MSM photodetector with interdigitated Schottky electrodes was then fabricated and characterized.

2 Experimental procedure

The epitaxial layers described in this work were grown by low pressure MOCVD in a vertical VEECO reactor. C-plane (0001) sapphire was employed as a substrate.

Received April 25, 2008; accepted July 14, 2008

E-mail: xywang@mail.semi.ac.cn

Trimethylaluminum (TMAl) and trimethylgallium (TMGa) were used as the group III precursors, while ammonia (NH_3) was used as the nitrogen source with purified H_2 as the carrier gas. Shown in Fig. 1 is a schematic diagram of the MOCVD-grown structure. First, a 25-nm-thick AlN buffer layer was deposited on the sapphire, followed by a 100-nm-thick high temperature (HT) $Al_xGa_{1-x}N$ template and ten pairs of HT AlN/$Al_xGa_{1-x}N$ SLs. Finally, a high Al content $Al_xGa_{1-x}N$ film with thickness of about 1 μm was grown at a high temperature. All $Al_xGa_{1-x}N$ layers had the same Al content, which was controlled by setting the deposition parameters. The growth temperature of the HT epilayers was kept at 1060ºC, and the sample was unintentionally doped.

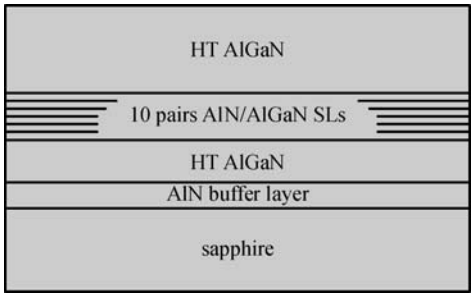

Fig. 1 Schematic diagram of low pressure MOCVD grown structure

An MSM photodetector was fabricated on the sample mentioned above using an interdigitated finger electrode. The fingers were designed to be 2 μm wide and 242 μm long, with 5 μm wide spacing. Immediately prior to the fabrication of metal electrodes, the wafer was dipped in the organic solution of acetone, and then ethanol, followed by deionized water to clean its surface. After lithographically patterning the interdigitated electrodes, a bi-layer Schottky metal of Ni/Au (3 nm/100 nm) was deposited and then lifted off. The active area was 250 μm×250 μm. Figure 2 shows an optical microscope top view of this device.

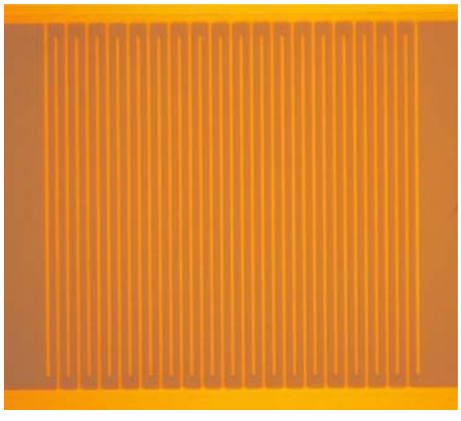

Fig. 2 Optical microscope top view of MSM photodetector

The device was measured under front illumination in a general opto-system with an Xe lamp filtered by a Jobin-Yvon H25 grating spectrometer, and the system was calibrated with a commercial UV-enhanced Si detector. The photocurrent was measured in direct current (DC) mode with a KEITHLEY 617 programmable electrometer. To minimize the effect of persistent photoconductivity (PPC), the spectral scan was performed from long wavelength to short wavelength. Responsivity was then calculated as the ratio of the photocurrent to the optical power incident on the detector.

3 Results and discussion

Shown in Fig. 3 is the high resolution X-ray diffraction (HRXRD) 2θ-ω scan for the sample. The prominent peak located at $2\theta = 35.35°$ is attributed to the top thick $Al_xGa_{1-x}N$ film. Using Vegard's law, Al content in the $Al_xGa_{1-x}N$ film can be estimated to be 54%. The rocking curve of the $Al_xGa_{1-x}N$ (0002) diffraction was also obtained (not shown in Fig. 3). The full width at half maximum (FWHM) of the ω scan curve for the $Al_{0.54}Ga_{0.46}N$ (0002) was about 597 arcsec, which is comparable with the result reported by Monroy et al. [21]. Furthermore, the FWHM of the ω scan curve for the $Al_{0.54}Ga_{0.46}N$ (10–12) was about 2311 arcsec. In the dissertation of Wang X L, a high Al content sample where FWHM of the ω scan curve for (0002) and (10–12) planes are 600 and 960 arcsec, respectively, is obtained [22]. In Fig. 3, the SLs 0-order, + 1-order, and −2-order peaks are distinguishable, and the −1-order is covered by the main peak. According to the relation $\Lambda=\lambda/(2\Delta\theta_M\cos\theta_B)$, where λ, θ_B, and $\Delta\theta_M$ are the X-ray wavelength, the Bragg angle of the superlattice 0-order satellite peak and the angle spacing between adjoining satellites, respectively [23], the period Λ of the SL is calculated to be 30 nm. Compared to the $Al_xGa_{1-x}N$ (0002) peak, the SL 0-order peak appears at a higher-angle position, indicating that the average Al

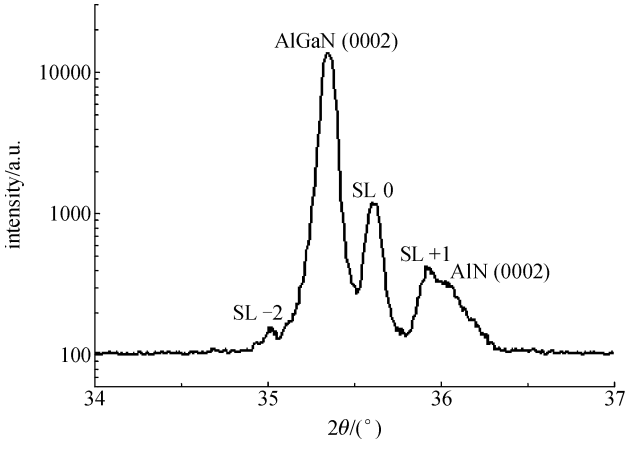

Fig. 3 HRXRD of the sample

content in the SL is larger than that in the top $Al_xGa_{1-x}N$ film. The $Al_xGa_{1-x}N$ film thus suffers a biaxial compression from the SL, which is considered to be effective to avoid wafer cracking. It should be noted that the in-plane biaxial compression in the $Al_xGa_{1-x}N$ film was not taken into account when estimating the Al mole fraction. If the strain is considered, the actual Al content will be a slightly higher than the estimated value of 54%.

Optical transmission measurement was performed before device fabrication. Shown in Fig. 4 is the transmittance spectrum, which was taken in the range of 200–800 nm using a PerkinElmer Lambda 950 UV/visible spectrometer with a cleaned sapphire substrate as reference. As seen from the figure, the cut-off wavelength is around 270 nm, confirming that our sample is suitable for fabricating a solar-blind photodetector. In the transmission region, the Fabry-Perot fringes are visible, indicating that high optical quality is obtained. As for the surface morphology of our sample, remarkable grain-like three-dimensional islands can be seen clearly according to the atomic force microscopy (AFM) results. The root mean square (RMS) surface roughness is about 18 nm.

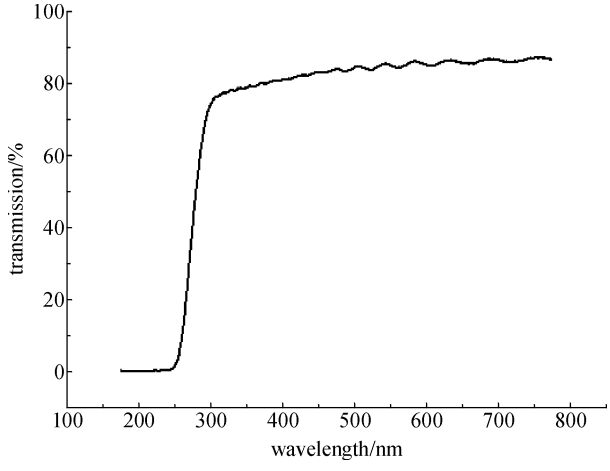

Fig. 4 Transmittance spectrum of the sample

Current-voltage (*I-V*) characteristics were measured using the KEITHLEY 617 programmable electrometer. The measured dark current of our solar-blind MSM photodetector is shown in Fig. 5 to be about 31 pA under a bias voltage of 5 V. It is clear that an MSM structure can be regarded as two Schottky contacts connected back-to-back. Under a certain bias voltage, one of the contacts is reverse-biased and the other is forward-biased. The *I-V* curve thus has a symmetrical "S" shape from – 10 to 10 V as shown in the inset of Fig. 5. Figure 6 shows the typical spectral response of the MSM device. An UV/visible contrast of about four orders of magnitude can be observed. However, the cutoff is not as abrupt as that obtained in GaN-based MSM photodetectors [24]. This may be caused by phase separation in the high Al content layer according to our previous research work [25]. Furthermore, the peak responsivity of our device at 250 nm is about 0.025 A/W. According to the relation $R = I_{photo}/P_\lambda = q\eta/(h\nu)$, where R is the responsivity, I_{photo} is the photocurrent, P_λ is the illumination power at wavelength λ (frequency ν), q is the absolute value of the electronic charge, and h is the Plank constant, respectively [26], the external quantum efficiency η corresponding to the peak responsivity is calculated to be 12.4%. The responsivity for the device as a function of the applied voltage is also shown in Fig. 6. It is observed that the responsivity increases with increments of the bias voltage, which has also been observed by other groups [27,28]. Currently, the dependence of the photocurrent and the responsivity on the bias has not been understood completely. Some researchers assume that the dependence can imply the existence of

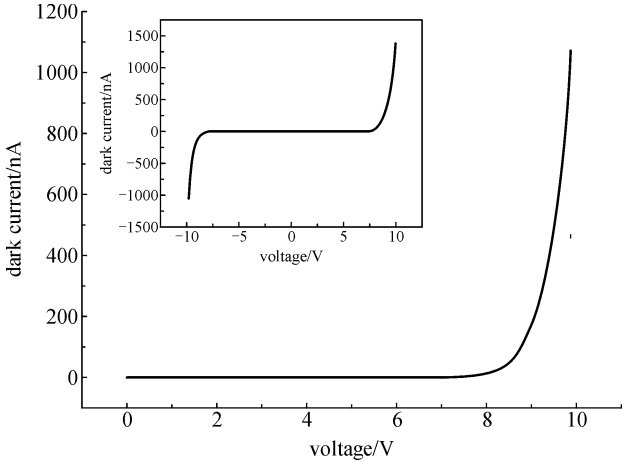

Fig. 5 Dark current of MSM photodetector at room temperature

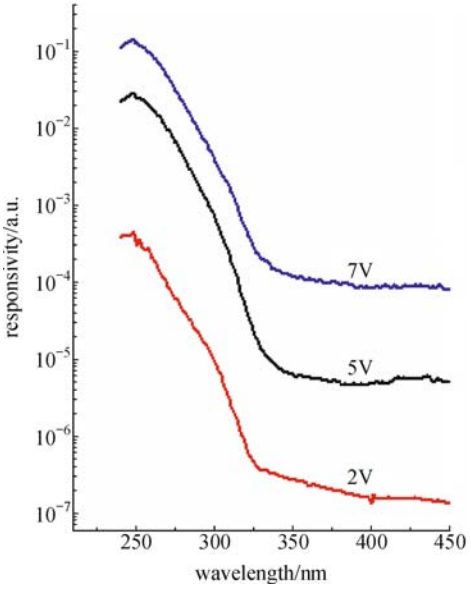

Fig. 6 Spectral response of MSM photodetector as a function of applied voltage

gain [29,30] and suggest that hole accumulation and image-force lowering induced by the surface states and defects at the depletion area account for the gain. However, these suggestions are uncertain and need further research [31,32].

4 Conclusion

The fabrication and characteristics of a solar-blind MSM photodetector based on 1 μm-thick $Al_{0.54}Ga_{0.46}N$ film grown by low pressure MOCVD have been reported. The dark current, responsivity and dependence of responsivity on the bias voltage have been measured. The detector has a low dark current of about 31 pA under a bias voltage of 5 V. An UV/visible contrast of about four orders of magnitude is observed, indicating that the spectral selectivity of the detector is fairly adequate.

Acknowledgements This work was supported by the Knowledge Innovation Engineering of Chinese Academy of Sciences (No. KGCX2-SW-107-1), the National Natural Science Foundation of China (Grant No. 60606002) and the State Key Development Program for Basic research of China (Nos. 2002CB311903, 2006CB604905, 513270505).

References

1. Kumakura K, Makimoto T. High-voltage operation with high current gain of pnp AlGaN/GaN heterojunction bipolar transistors with thin n-type GaN base. Applied Physics Letters, 2005, 86(2): 023506-1–023506-3
2. Liu Y, Egawa T, Jiang H, Zhang B J, Ishikawa H. Novel quaternary AlInGaN/GaN heterostructure field effect transistors on sapphire substrate. Japanese Journal of Applied Physics, 2006, 45(7): 5728–5731
3. Wang X L, Wang C M, Hu G X, Wang J X, Chen T S, Jiao G, Li J P, Zeng Y P, Li J M. Improved DC and RF performance of AlGaN/GaN HEMTs grown by MOCVD on sapphire substrates. Solid-State Electronics, 2005, 49(8): 1387–1390
4. Wang X L, Wang C M, Hu G X, Xiao H L, Fang C B, Wang J X, Ran J X, Li J P, Li J M, Wang Z G. MOCVD-grown high-mobility $Al_{0.3}Ga_{0.7}N$/AlN/GaN HEMT structure on sapphire substrate. Journal of Crystal Growth, 2007, 298: 791–793
5. Wang X L, Hu G X, Ma Z Y, Ran J X, Wang C M, Xiao H L, Tang J, Li J P, Wang J X, Zeng Y P, Li J M, Wang Z G. AlGaN/AlN/GaN/SiC HEMT structure with high mobility GaN thin layer as channel grown by MOCVD. Journal of Crystal Growth, 2007, 298: 835–839
6. Wang X L, Cheng T S, Ma Z Y, Hu G X, Xiao H L, Ran J X, Wang C M, Luo W J. 1-mm gate periphery AlGaN/AlN/GaN HEMTs on SiC with output power of 9.39 W at 8 GHz. Solid-State Electronics, 2007, 51(3): 428–432
7. Wang X L, Wang C M, Hu G X, Wang J X, Li J P. Room temperature mobility above 2100 cm^2/Vs in $Al_{0.3}Ga_{0.7}N$/AlN/GaN heterostructures grown on sapphire substrates by MOCVD. Physica Status Solidi C, 2006, 3(3): 607–610
8. Wang X L, Chen T S, Xiao H L, Wang C M, Hu G X, Luo W J, Tang J, Guo L C, Li J M. High-performance 2 mm gate width GaN HEMTs on 6H-SiC with output power of 22.4 W @ 8 GHz. Solid-State Electronics, 2008, 52(6): 926–929
9. Nakamura S, Mukai T, Senoh M. Candela-class high-brightness InGaN/AlGaN double-heterostructure blue-light-emitting diodes. Applied Physics Letters, 1994, 64(13): 1687–1689
10. Nakamura S, Senoh M, Nagahama S, Iwasa N, Yamada T, Matsushita T, Kiyoku H, Sugimoto Y, Kozaki T, Umemoto H, Sano M, Chocho K. InGaN/GaN/AlGaN-based laser diodes with modulation-doped strained-layer superlattices grown on an epitaxially laterally overgrown GaN substrate. Applied Physics Letters, 1998, 72(2): 211–213
11. Adivarahan V, Wu S, Zhang J P, Chitnis A, Shatalov M, Mandavilli V, Gaska R, Khan M A. High-efficiency 269 nm emission deep ultraviolet light-emitting diodes. Applied Physics Letters, 2004, 84(23): 4762–4764
12. Nishida T, Saito H, Kobayashi N. Efficient and high-power AlGaN-based ultraviolet light-emitting diode grown on bulk GaN. Applied Physics Letters, 2001, 79(6): 711–712
13. Martin R W, Edwards P R, Pecharroman-Gallego R, Liu C, Deatcher C J, Watson I M, O'Donnell K P. Light emission ranging from blue to red from a series of InGaN/GaN single quantum wells. Journal of Physics D: Applied Physics, 2002, 35(7): 604–608
14. Walker D, Kumar V, Mi K, Sandvik P, Kung P, Zhang X H, Razeghi M. Solar-blind AlGaN photodiodes with very low cutoff wavelength. Applied Physics Letters, 2000, 76(4): 403–405
15. Sandvik P, Walker D, Kung P, Mi K, Shahedipour F, Kumar V, Zhang H, Diaz J, Jelen C, Razeghi M. Solar-blind $Al_xGa_{1-x}N$ p-i-n photodetectors grown on LEO and non-LEO GaN. Proceedings of SPIE, 2000, 3948: 265–272
16. Lambert D J H, Wong M M, Chowdhury U, Collins C, Li T, Kwon H K, Shelton B S, Zhu T G, Campbell J C, Dupuis R D. Back illuminated AlGaN solar-blind photodetectors. Applied Physics Letters, 2000, 77(12): 1900–1902
17. Brown J D, Li J, Srinivasan P, Matthews J, Schetzina J F. Solar-blind AlGaN heterostructure photodiodes. MRS Internet Journal of Nitride Semiconductor Research, 2000, 5: 9
18. Tarsa E J, Kozodoy P, Ibbetson J, Keller B P, Parish G, Mishra U. Solar-blind AlGaN-based inverted heterostructure photodiodes. Applied Physics Letters, 2000, 77(3): 316–318
19. Duboz J Y, Grandjean N, Dussaigne A, Mosca M, Reverchon J L, Verly P G, Simpson R H. Solar blind AlGaN photodetectors with a very high spectral selectivity. The European Physical Journal — Applied Physics, 2006, 33(1): 5–7
20. Keller S, Denbaars S P. Metalorganic chemical vapor deposition of group III nitrides: a discussion of critical issues. Journal of Crystal Growth, 2003, 248(1–4): 479–486
21. Monroy E, Daudin B, Bellet-Amalric E, Gogneau N, Jalabert D, Enjalbert F, Brault J, Barjon J, Dang L S. Surfactant effect of In for AlGaN growth by plasma-assisted molecular beam epitaxy. Journal of Applied Physics, 2003, 93(3): 1550–1556
22. Wang X L. Investigations on the epitaxial growth and characteristics of AlGaN with high Al content via metalorganic chemical vapor deposition. Dissertation for the Doctoral Degree. Beijing: Institute of Semiconductors, 2007, 25
23. Bowen D K, Tanner B K. High Resolution X-Ray Diffractometry

and Topography. Padstow: CRC Press, 1998, 64

24. Palacios T, Monroy E, Calle F, Omnès F. High-responsivity submicron metal-semiconductor-metal ultraviolet detectors. Applied Physics Letters, 2002, 81(10): 1902–1904
25. Wang X Y, Wang X L, Hu G X, Wang B Z, Ma Z Y, Xiao H L, Wang C M, Ran J X, Li J P. Characteristics of high Al content $Al_xGa_{1-x}N$ grown by metalorganic chemical vapor deposition. Microelectronics Journal, 2007, 38(8–9): 838–841
26. Parish G. Growth and characterization of aluminum gallium nitride/gallium nitride ultraviolet detectors. Dissertation for the Doctoral Degree. Santa Barbara: University of California, 2001, 12
27. Pau J L, Monroy E, Munoz E, Calle F, Sanchez-Garcia M A, Calleja E. Fast AlGaN metal-semiconductor-metal photodetectors grown on Si(111). Electronics Letters, 2001, 37(4): 239–240
28. Lee I H. Low dark current Schottky metal-semiconductor-metal photodetectors fabricated on AlGaN epitaxial layers for visible-blind ultraviolet detection. Physica Status Solidi A, 2002, 192(1): R4–R6
29. Osinsky A, Gangopadhyay S, Yang J W, Gaska R, Kuksenkov D, Temkin H, Shmagin I K, Chang Y C, Muth J F, Kolbas R M. Visible-blind GaN Schottky barrier detectors grown on Si(111). Applied Physics Letters, 1998, 72(5): 551–553
30. Carrano J C, Grudowski P A, Eiting C J, Dupuis R D, Campbell J C. Current transport mechanisms in GaN-based metal-semiconductor-metal photodetectors. Applied Physics Letters, 1998, 72(5): 542–544
31. Burm J, Eastman L F. Low-frequency gain in MSM photodiodes due to charge accumulation and image force lowering. IEEE Photonics Technology Letters, 1996, 8(1): 113–115
32. Katz O, Garber V, Meyler B, Bahir G, Salzman J. Gain mechanism in GaN Schottky ultraviolet detectors. Applied Physics Letters, 2001, 79(10): 1417–1419